Title

A spurious jump in the satellite record: Has Antarctic sea ice expansion been overestimated?

Journal

Cryosphere, 8(4)

ISSN

1994-0416

Authors

Eisenman, I
Meier, WN
Norris, JR

Publication Date

2014-07-22

DOI

10.5194/tc-8-1289-2014

Peer reviewed

The Cryosphere, 8, 1289–1296, 2014
www.the-cryosphere.net/8/1289/2014/
doi:10.5194/tc-8-1289-2014

The Cryosphere
Open Access

A spurious jump in the satellite record: has Antarctic sea ice expansion been overestimated?

I. Eisenman[1], **W. N. Meier**[2], **and J. R. Norris**[1]

[1]Scripps Institution of Oceanography, University of California at San Diego, La Jolla, CA, USA
[2]NASA Goddard Space Flight Center, Greenbelt, MD, USA

Correspondence to: I. Eisenman (eisenman@ucsd.edu)

Received: 21 December 2013 – Published in The Cryosphere Discuss.: 13 January 2014
Revised: 4 July 2014 – Accepted: 5 July 2014 – Published: 22 July 2014

Abstract. Recent estimates indicate that the Antarctic sea ice cover is expanding at a statistically significant rate with a magnitude one-third as large as the rapid rate of sea ice retreat in the Arctic. However, during the mid-2000s, with several fewer years in the observational record, the trend in Antarctic sea ice extent was reported to be considerably smaller and statistically indistinguishable from zero. Here, we show that much of the increase in the reported trend occurred due to the previously undocumented effect of a change in the way the satellite sea ice observations are processed for the widely used Bootstrap algorithm data set, rather than a physical increase in the rate of ice advance. Specifically, we find that a change in the intercalibration across a 1991 sensor transition when the data set was reprocessed in 2007 caused a substantial change in the long-term trend. Although our analysis does not definitively identify whether this change introduced an error or removed one, the resulting difference in the trends suggests that a substantial error exists in either the current data set or the version that was used prior to the mid-2000s, and numerous studies that have relied on these observations should be reexamined to determine the sensitivity of their results to this change in the data set. Furthermore, a number of recent studies have investigated physical mechanisms for the observed expansion of the Antarctic sea ice cover. The results of this analysis raise the possibility that much of this expansion may be a spurious artifact of an error in the processing of the satellite observations.

1 Introduction

Observational estimates of the sea ice cover in both hemispheres are available at approximately daily resolution from satellite passive microwave measurements from the late 1970s onwards. The microwave emissivity of sea ice is typically higher than that of the ocean, causing ice-covered regions to emit with greater intensity (i.e., have a higher brightness temperature) than regions with an ice-free ocean surface of the same temperature. Because warmer surfaces also emit with higher intensity, however, it is difficult to distinguish between cold sea ice and a warm ice-free ocean surface using brightness temperature measurements at a single frequency and polarization. Hence simultaneous measurements at multiple frequencies and polarizations are normally used to estimate the sea ice concentration (i.e., the fraction of each ocean pixel that is covered with ice), because the difference in emissivity between sea ice and open ocean varies as a function of frequency and polarization. A suite of other issues further complicate estimates of sea ice concentration from passive microwave data, including interference from weather effects; the similarity in microwave emissivity between sea ice and regions within a sensor footprint containing both land and ice-free ocean; and the similarity in microwave emissivity between ice-free ocean, melt ponds on thick ice floes, and thin ice (e.g., Maslanik, 1992; Cavalieri et al., 1995).

Two separate algorithms for estimating sea ice concentrations from passive microwave satellite measurements of brightness temperatures at multiple frequencies and polarizations were developed concurrently in the 1980s at the NASA Goddard Space Flight Center. Both algorithms are physically motivated but highly empirical in their implementation. The

Published by Copernicus Publications on behalf of the European Geosciences Union.

first, called the "Bootstrap" algorithm, is based on interpolation between clusters of points in scatter plots of brightness temperatures (Comiso, 1986) (note that it does not involve the statistical bootstrapping technique). The second, called the "NASA Team" algorithm, is based on difference ratios between brightness temperatures (Cavalieri et al., 1984). Here we focus on the Bootstrap algorithm, which is one of the most widely used ice concentration products and forms the basis of the discussion of observed sea ice changes in the Intergovernmental Panel on Climate Change Fourth Assessment Report (IPCC AR4) (IPCC, 2007) and Fifth Assessment Report (IPCC AR5) (IPCC, 2013).

In recent years, there has been substantial interest in the trend in Antarctic sea ice extent (i.e., the sum of the surface areas of all grid cells that have an ice concentration above 15 %) primarily due to the observed asymmetry between increasing ice extent in the Antarctic and rapidly diminishing ice extent in the Arctic (e.g., Cavalieri et al., 1997) and the inability of current climate models to capture this (e.g., Eisenman et al., 2011).

The IPCC AR5 reported the observed Antarctic sea ice extent to be expanding at a highly statistically significant rate (monthly anomalies from the mean seasonal cycle increasing at $16.5 \pm 3.5 \times 10^3\,\mathrm{km}^2\,\mathrm{yr}^{-1}$), with a magnitude one-third as large as the sea ice retreat in the Arctic ($-48.0 \pm 3.0 \times 10^3\,\mathrm{km}^2\,\mathrm{yr}^{-1}$). This is in substantial contrast with the IPCC AR4, which reported the trend in Antarctic sea ice extent to be small and statistically indistinguishable from zero ($5.6 \pm 9.2 \times 10^3\,\mathrm{km}^2\,\mathrm{yr}^{-1}$; see Appendix A). The Antarctic sea ice extent trend was highlighted as a bullet point in the *Summary for Policymakers* of both the IPCC AR4 and IPCC AR5, and the substantial increase in this trend is one of the notable differences between the two reports.

The contrast in trend is also apparent in the literature preceding each IPCC report, with a modest Antarctic sea ice extent trend reported in the early 2000s (Comiso and Steffen, 2001; Comiso, 2003), and reported trends that were considerably larger in later papers that used ostensibly nearly the same data set with several additional years of observations (Comiso and Nishio, 2008; Comiso, 2010) (see details in Appendix A).

This change in the trend has generally been attributed within the community to the lengthening time span and associated addition of new data. However, the results presented below demonstrate that much of the change in the trend actually occurred due to the previously undocumented effect of a change in the Bootstrap sea ice data set in the late 2000s.

2 Data

The data and methods are summarized here and described in detail in Sect. S1 in the Supplement. We analyze daily Bootstrap sea ice concentration fields for the time period November 1978 through December 2012, which are available for public download from the National Snow and Ice Data Center (NSIDC) (Comiso, 2000). In September 2007, NSIDC documented an update to the Bootstrap algorithm for consistency with other satellite measurements (see Sect. S1.3 in the Supplement), and the entire data set was reprocessed. NSIDC refers to the current data set as "Version 2", a convention we follow here. This update to the data set was generally viewed within the community as having a negligible impact on the trend (Comiso and Nishio, 2008).

We also analyze the version of the data set that was posted on the NSIDC website prior to the September 2007 version update, which we acquired from NSIDC User Services, and we refer to this earlier data set as "Version 1". This data set covers the time period November 1978 through December 2004. We calculate a monthly ice extent time series from each of the two ice concentration data sets.

For comparison with studies published previously, we truncate each data set at a range of endpoints and calculate the trend. We follow the standard practice for estimating trends in the ice cover by using ordinary least squares linear regression of monthly anomalies from the mean seasonal cycle, with the regression confidence interval being treated as an error bar that accounts for uncertainty associated with natural variability about the linear trend (e.g., Parkinson et al., 1999). We note that this method assumes that the trend is linear in time and that natural variability can be treated as white noise drawn from a zero-mean normal distribution. It should be emphasized that the error bar constructed in this way does not include any uncertainty associated with the satellite retrieval, which the results of this study suggest may expand the error bar considerably. Although superior measures of error could be identified, here we follow this standard convention. Hence for each endpoint (computed for every month), anomalies are computed with respect to the mean seasonal cycle averaged over all months in the truncated record, and then the trend estimate and confidence interval for the anomaly time series are calculated.

3 Results and discussion

The time series of annual-mean ice extent anomalies for both versions of the Bootstrap data set are plotted in Fig. 1a. There is a readily discernible bias between the two versions of the Bootstrap data set. Although both versions have similar values for each year, Version 2 has slightly lower values before 1991 and slightly higher values afterward. This is associated with a substantial difference in the 1979–2004 trend (dashed lines in Fig. 1a), implying that studies using Version 2 of the Bootstrap data set will estimate larger rates of expansion of the Antarctic sea ice cover.

In order to assess how this issue influences how the published trend has evolved during the past decade, we vary the endpoint in each version of the Bootstrap record and then compute the trend (Fig. 1b). For all plotted endpoints,

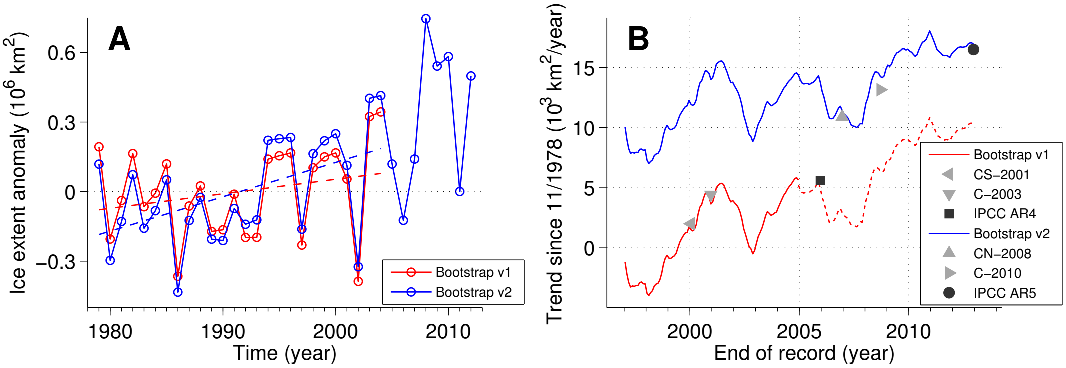

Figure 1. Antarctic sea ice extent calculated with the current Bootstrap data set (Version 2, blue), as well as an ostensibly nearly equivalent version of the data set that was distributed previously (Version 1, red). **(A)** Annual-mean ice extent anomalies from the 1979–2004 mean. Trends for the two annual time series, calculated for the period 1979–2004, are indicated by dashed lines. **(B)** Trends in the monthly-mean ice extent records truncated at a range of endpoints (curves) and compared with values published previously (symbols). Trends reported in the literature, which are plotted above the end date of the data set considered in each study, are from four studies (Comiso and Steffen, 2001; Comiso, 2003; Comiso and Nishio, 2008; Comiso, 2010), the IPCC AR4 (IPCC, 2007), and the IPCC AR5 (IPCC, 2013) (see Appendix A). The red dashed line is an approximate continuation of the Version 1 data set using Version 1B (see Sect. 3). Values published in the early to mid-2000s align with the Bootstrap Version 1 curve, and values published more recently align with the Bootstrap Version 2 curve.

Version 2 (blue curve) has a substantially larger positive trend than Version 1 (red curve).

Previously published values for the trend in Antarctic sea ice extent are plotted in Fig. 1b (symbols) above the end date of the record that was analyzed in each study. The trends reported in the IPCC AR4 and papers published before it match the values computed here using Version 1, whereas the trends reported in later papers and the IPCC AR5 match the substantially higher values computed here using Version 2. Similarly, an earlier study that analyzed data through 1998 reported that the Bootstrap algorithm produced "a small negative trend for ice extent" in the Antarctic (Zwally et al., 2002), which is consistent with Version 1 in Fig. 1b.

Although there is some variability in the red and blue curves in Fig. 1b, it is clear that much of the change in the reported trend between the IPCC AR4 (black square) and IPCC AR5 (black circle) is due to the transition from Version 1 to Version 2. Specifically, if the Version 2 data set had been used in the IPCC AR4 analysis of ice extent during 1979–2005, the trend would have been $14.1 \times 10^3\,\mathrm{km}^2\,\mathrm{yr}^{-1}$, a value fairly similar to the trend of $16.5 \times 10^3\,\mathrm{km}^2\,\mathrm{yr}^{-1}$ reported in the IPCC AR5 analysis of 1979–2012 and in marked contrast with the trend of $5.6 \times 10^3\,\mathrm{km}^2\,\mathrm{yr}^{-1}$ that was reported in the IPCC AR4 based on Version 1 data. Overall, we find that most of the increase in trend between the IPCC AR4 and AR5 is associated with the update from Version 1 to Version 2, with the remainder being due to the additional years in the record (see Table S1 in the Supplement).

The two data sets can be compared to determine the temporal structure of the difference between them. The difference in ice extent between Version 2 and Version 1 is plotted in Fig. 2. There is a clear transition in December 1991, which coincides with a satellite sensor change (vertical dashed line; see Sect. S1.1 in the Supplement): on 3 December 1991, there was a transition from the Special Sensor Microwave/Imager (SSM/I) flown on the Defense Meteorological Satellite Program (DMSP) F8 satellite to the SSM/I flown on the DMSP F11 satellite. Version 2 has a smaller value in nearly all months prior to the sensor change and a larger value in nearly all months after it.

This implies that the 2007 update of the entire data set from Version 1 to Version 2 included a substantial change in the intercalibration across the December 1991 sensor transition. Hence the difference in trend between the two curves in Fig. 1b appears to be associated with an erroneous sensor change intercalibration in one of the two Bootstrap versions.

Although an update to the Bootstrap algorithm was documented on the NSDIC website (see Sect. S1.3 of Supplement) and we compare the data set before (Version 1) and after (Version 2) this update occurred, we cannot be certain that the two data sets we analyze contain only the differences discussed in the documented update for several reasons. First, there is some ambiguity in the Bootstrap data set version control. For example, we find that the "original" data set discussed in Comiso and Nishio (2008) coincides with our Version 2 data set, implying that the salient change in the data set preceded the analysis in Comiso and Nishio (2008), which is the paper typically cited for the version update. Further ambiguities in the documentation of the Bootstrap version update are discussed in Sect. S1.3 of the Supplement. Second, the Bootstrap algorithm uses brightness temperature measurements which are processed by Remote Sensing Systems, and the version has changed over time due to new temperature calibrations and corrections of small errors. However, this is unlikely to be the source of the jump in December 1991, because intercalibration across sensor changes

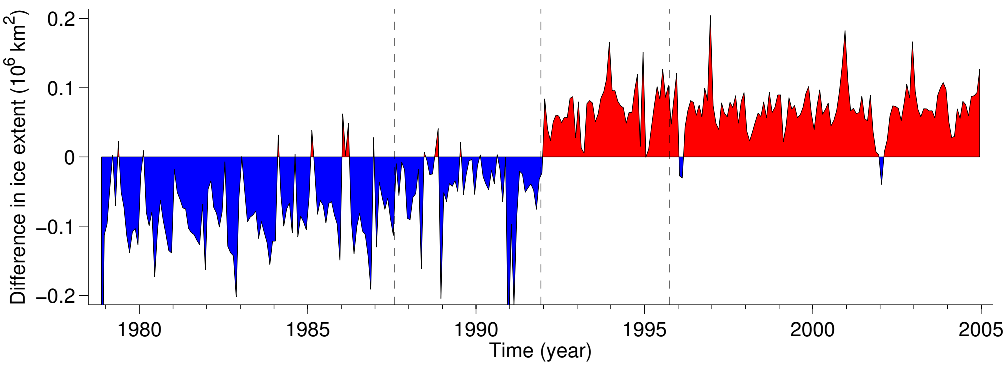

Figure 2. Difference between sea ice extents in the two Bootstrap data sets, plotted as Version 2 − Version 1. Both records are monthly-mean anomalies from the 1979–2004 mean seasonal cycle. Transitions between satellite sensors are indicated by vertical dashed lines (see Sect. S1.1 in the Supplement). The difference in ice extent appears to be dominated by a spurious jump in one of the data sets coinciding with the December 1991 sensor transition.

occurs at the algorithm level through the adjustment of algorithm coefficients (tie points), and this should account for any basic inconsistency in brightness temperatures across a sensor change.

To the extent that Fig. 2 resembles a step function, we can generate an approximate extension of Version 1 by subtracting a constant offset from Version 2 after the sensor change. We refer to this time series as "Version 1B", which we generate by subtracting 0.16×10^6 km^2 from Version 2 in all months after December 1991. Whereas the Version 1 data set ends in December 2004, Version 1B spans the longer time period from November 1978 through December 2012 (the same time period as Version 2). Version 1B has a trend that is nearly equivalent to Version 1 for the range of endpoints plotted in Fig. 1b (see Fig. S5c in the Supplement), and it is used to approximately extend Version 1 for comparison with Version 2 (red dashed line in Fig. 1b; see also Table S1 in the Supplement).

In the Supplement (Sect. S2), several methods are investigated to identify whether the change from Version 1 to Version 2 introduced an error or removed one. None of these methods unequivocally resolves the issue. Specifically, we compare the two Bootstrap versions with ice extents computed using the NASA Team algorithm, examine the temporal and spatial features of the differences between data sets, and also consider the Arctic sea ice cover in the three data sets. The main findings discussed in Sect. S2 include (1) that the difference between the NASA Team data set and each Bootstrap version is too noisy to definitively identify which Bootstrap version has an error (Fig. S2); (2) that there also appear to be differences in the Arctic between the two Bootstrap versions as well as the NASA Team data set across some sensor changes (Fig. S4); (3) that the differences in trend between the two Bootstrap data sets and the NASA Team data set in both the Antarctic and the Arctic are considerably larger than the error bar that typically accompanies reported trend estimates (Figs. S5–S8), implying that the regression confidence interval substantially underestimates the uncertainty in the sea ice trends by failing to account for errors associated with the ice concentration retrieval; (4) that there was also a change in the Arctic sea ice extent trend associated with the Bootstrap data set update, but it was relatively small compared with the real change in trend associated with adding several more years to the record between the IPCC AR4 and IPCC AR5 (Fig. S7); (5) that there is little overall seasonal structure in the Antarctic sea ice trend in any of the records (Fig. S9); and (6) that the spatial structure of the difference in Antarctic sea ice concentration between the two Bootstrap versions appears to be relatively spatially uniform, consistent with an error in the intercalibration across a sensor change (Fig. S11).

4 Conclusions

In summary, we find that much of the large increase in the reported rate of Antarctic sea ice expansion since the IPCC AR4 occurred due to the previously undocumented effect of a change in the way the observations are processed, rather than being simply due to the addition of several years of data. Specifically, we find that the current Bootstrap Antarctic sea ice extent data set (Version 2) produces substantially larger trends for a given time period than the ostensibly nearly identical data set used prior to 2007 (Version 1). We are able to reproduce the results of pre-2007 studies and the IPCC AR4 using the Version 1 data set and to reproduce the results of more recent studies and the IPCC AR5 using the Version 2 data set, and we demonstrate the difference in the trend by comparing the two data sets. We find that the cause of the difference in the trend is a previously undocumented change in the intercalibration across a 1991 sensor transition when the data set was reprocessed in 2007.

With the lack of a more precise version control for the Bootstrap sea ice concentration data set (see Sect. S1.3 in the Supplement), it is difficult to determine exactly what caused this change in the trend. Importantly, there was no documentation of any change in the Bootstrap data set directly influencing the intercalibration across the sensor transition in December 1991. Hence we cannot be certain whether the change that caused the increase in the trend corrected a problem or introduced one, and we lay out two possibilities that are consistent with the results of this analysis. The first possibility is that Version 1 is approximately correct, and a spurious jump in 1991 from a sensor transition intercalibration error was inadvertently introduced into the Bootstrap data set in the 2007 update from Version 1 to Version 2. In this case, the rate of Antarctic sea ice expansion has been overestimated in recent years, and recent literature including the IPCC AR5 *Summary for Policymakers* contains an error that needs to be corrected. The second possibility is that Version 2 is approximately correct, and a spurious jump in 1991 from a sensor transition intercalibration error that existed in Version 1 was corrected in the 2007 update to Version 2, although this correction was never explicitly documented. In this case, earlier literature including the IPCC AR4 *Summary for Policymakers* contains a previously undocumented error, and the substantial body of science generated prior to 2007 that relied on Bootstrap Antarctic sea ice concentration to reach its conclusions needs to be reexamined to assess how this correction to the data set influences the results of the studies.

We note that while we focus here on the Bootstrap data set, which was the source for the conclusions in the IPCC AR4 and IPCC AR5, such issues can arise in other satellite sea ice data sets (or any climate data record) due to factors including inconsistencies in source data, changes in processing method, and the addition of new data sources (e.g., Screen, 2011).

A number of studies have proposed physical mechanisms for the reported expansion of the Antarctic sea ice cover during recent decades. The ozone hole was suggested as a possible cause (Thompson and Solomon, 2002; Turner et al., 2009), but recent modeling studies have found that Antarctic ozone depletion causes sea ice retreat rather than advance (Sigmond and Fyfe, 2010; Bitz and Polvani, 2012). Other studies have proposed more ice growth associated with a stronger halocline due to increased freshwater flux from ice sheet discharge (Bintanja et al., 2013) or precipitation (Liu and Curry, 2010), less ice melt from a weakened ocean heat flux associated with stronger ocean stratification (Zhang, 2007), or suppressed warming due to ocean heat uptake (Kirkman and Bitz, 2011), although an observational analysis suggests that the ice cover changes have been driven primarily by winds (Holland and Kwok, 2012). Natural variability has also been suggested as the cause (Zunz et al., 2013; Polvani and Smith, 2013), although this requires a relatively low probability event to be occurring. The results of this analysis raise an alternative and potentially complementary possibility. If Version 1 is approximately correct and Version 2 contains an error, then much of the apparent sea ice growth in the Southern Hemisphere is a spurious artifact in the satellite record.

These results illustrate the need for thorough documentation and version control in observational data sets. Ideally all observational data sets, especially those used widely and included in IPCC assessment reports, would have sufficient documentation of algorithms and algorithm changes for previous and current versions of the data to be independently replicated from the raw sensor data. Such transparency is particularly essential for highly visible and at times controversial climate change parameters such as the sea ice cover.

Appendix A: Previously published trends

Here we summarize the Bootstrap Antarctic sea ice extent trends reported in previous publications that are included as symbols in Fig. 1b.

A series of papers have reported trends computed using monthly-mean Bootstrap ice extent anomalies from the mean seasonal cycle including error bars that represent the 68 % linear regression confidence interval. All used records that begin in either November 1978 or January 1979 but end at different times. With data until January 2000, the trend was reported to be $2.0 \pm 3.9 \times 10^3\ \mathrm{km}^2\ \mathrm{yr}^{-1}$ (Comiso and Steffen, 2001); with data until December 2000, the trend was reported to be $4.4 \pm 3.7 \times 10^3\ \mathrm{km}^2\ \mathrm{yr}^{-1}$ (Comiso, 2003); with data until December 2006, the trend was reported to be $10.9 \pm 2.7 \times 10^3\ \mathrm{km}^2\ \mathrm{yr}^{-1}$ (Comiso and Nishio, 2008); and with data until September 2008, the trend was reported to be $13.2 \pm 2.5 \times 10^3\ \mathrm{km}^2\ \mathrm{yr}^{-1}$ (Comiso, 2010).

The IPCC AR4, which used annual-mean Bootstrap data during 1979–2005 and an error bar representing the 90 % linear regression confidence interval, reported the trend in Antarctic sea ice extent to be $5.6 \pm 9.2 \times 10^3\ \mathrm{km}^2\ \mathrm{yr}^{-1}$. This point is included in Fig. 1b above December 2005 (see also Table S1 in the Supplement). The IPCC AR4 *Summary for Policymakers* reported that Antarctic sea ice showed "no statistically significant average trends".

The IPCC AR5, which used monthly-mean Bootstrap data during November 1978 through December 2012 and an error bar representing the 90 % linear regression confidence interval, reported the trend in Antarctic sea ice extent to be $16.5 \pm 3.5 \times 10^3\ \mathrm{km}^2\ \mathrm{yr}^{-1}$ (see also Table S1 in the Supplement), with the uncertainty range being included in the IPCC AR5 *Summary for Policymakers*.

The slight differences in Fig. 1b between previously reported trends (symbols) and those computed here (curves) are expected to arise due to issues including rounding errors associated with the number of significant figures used to report trends, slight differences in the data sets, and slight differences in the methodology such as how missing data are treated and how ice extent is calculated from the gridded ice concentration fields.

The Supplement related to this article is available online at doi:10.5194/tc-8-1289-2014-supplement.

Acknowledgements. We thank the editor, R. Lindsay, for helpful suggestions that improved the final presentation, as well as K. Cowtan, G. Foster, P. Holland, E. Steig, J. Walsh, and an anonymous reviewer for raising a number of useful points in the online discussion of this paper. Without implying that they endorse our results, we also thank B. Cornuelle, H. Fricker, J. Comiso, T. Merlis, B. Rose, H. Stern, T. Martin, T. Wagner, M.-L. Timmermans, J. S. Wettlaufer, and J. Walsh for helpful discussions. This work was supported by NSF grant ARC-1107795 and the G. Unger Vetlesen Foundation.

Edited by: R. Lindsay

References

Bintanja, R., van Oldenborgh, G. J., Drijfhout, S. S., Wouters, B., and Katsman, C. A.: Important role for ocean warming and increased ice-shelf melt in Antarctic sea-ice expansion, Nat. Geosci., 6, 376–379, doi:10.1038/NGEO1767, 2013.

Bitz, C. M. and Polvani, L. M.: Antarctic climate response to stratospheric ozone depletion in a fine resolution ocean climate model, Geophys. Res. Lett., 39, L20705, doi:10.1029/2012GL053393, 2012.

Cavalieri, D. J., Gloersen, P., and Campbell, W. J.: Determination of sea ice parameters with the Nimbus-7 SMMR, J. Geophys. Res., 89, 5355–5369, doi:10.1029/JD089iD04p05355, 1984.

Cavalieri, D. J., St. Germain, K. M., and Swift, C. T.: Reduction of weather effects in the calculation of sea-ice concentration with the DMSP SSM/I, J. Glaciol., 41, 455–464, 1995.

Cavalieri, D. J., Gloersen, P., Parkinson, C. L., Comiso, J. C., and Zwally, H. J.: Observed hemispheric asymmetry in global sea ice changes, Science, 278, 1104–1106, 1997.

Comiso, J. C.: Characteristics of arctic winter sea ice from satellite multispectral microwave observations, J. Geophys. Res., 91, 975–994, doi:10.1029/JC091iC01p00975, 1986.

Comiso, J. C.: Bootstrap Sea Ice Concentrations from Nimbus-7 SMMR and DMSP SSM/I-SSMIS. Version 2, Updated 2012, National Snow and Ice Data Center, Boulder, CO, USA, available at: http://nsidc.org/data/nsidc-0079.html (last access: 30 September 2013), 2000.

Comiso, J. C.: Large scale characteristics and variability of the global sea ice cover, in: Sea Ice – An Introduction to its Physics, Biology, Chemistry and Geology, Blackwell Scientific Ltd., Oxford, UK, 112–142, 2003.

Comiso, J. C.: Variability and trends of the global sea ice cover, in: Sea Ice, 2nd edn., Wiley-Blackwell, Oxford, UK, 205–246, 2010.

Comiso, J. C. and Nishio, F.: Trends in the sea ice cover using enhanced and compatible AMSR-E, SSM/I, and SMMR data, J. Geophys. Res., 113, C02S07, doi:10.1029/2007JC004257, 2008.

Comiso, J. C. and Steffen, K.: Studies of Antarctic sea ice concentrations from satellite data and their applications, J. Geophys. Res., 106, 31361–31385, doi:10.1029/2001JC000823, 2001.

Eisenman, I., Schneider, T., Battisti, D. S., and Bitz, C. M.: Consistent changes in the sea ice seasonal cycle in response to global warming, J. Climate, 24, 5325–5335, doi:10.1175/2011JCLI4051.1, 2011.

Holland, P. R. and Kwok, R.: Wind-driven trends in Antarctic sea-ice drift, Nat. Geosci., 5, 872–875, doi:10.1038/NGEO1627, 2012.

IPCC: Climate Change 2007: The Physical Science Basis. Contribution of Working Group I to the Fourth Assessment Report of the Intergovernmental Panel on Climate Change, edited by: Solomon, S., Qin, D., Manning, M., Chen, Z., Marquis, M., Averyt, K. B., Tignor, M., and Miller, H. L., Cambridge University Press, Cambridge, United Kingdom and New York, NY, USA, 2007.

IPCC: Climate Change 2013: The Physical Science Basis. Contribution of Working Group I to the Fifth Assessment Report of the Intergovernmental Panel on Climate Change, edited by: Stocker, T. F., Qin, D., Plattner, G.-K., Tignor, M., Allen, S. K., Boschung, J., Nauels, A., Xia, Y., Bex, V., and Midgley, P. M., Cambridge University Press, Cambridge, United Kingdom and New York, NY, USA, 2013.

Kirkman, C. H. and Bitz, C. M.: The effect of the sea ice freshwater flux on Southern Ocean temperatures in CCSM3: deep-ocean warming and delayed surface warming, J. Climate, 24, 2224–2237, doi:10.1175/2010JCLI3625.1, 2011.

Liu, J. P. and Curry, J. A.: Accelerated warming of the Southern Ocean and its impacts on the hydrological cycle and sea ice, P. Natl. Acad. Sci. USA, 107, 14987–14992, doi:10.1073/pnas.1003336107, 2010.

Maslanik, J. A.: Effects of weather on the retrieval of sea ice concentration and ice type from passive microwave data, Int. J. Remote Sens., 13, 37–54, 1992.

Parkinson, C. L., Cavalieri, D. J., Gloersen, P., Zwally, H. J., and Comiso, J. C.: Arctic sea ice extents, areas, and trends, 1978–1996, J. Geophys. Res., 104, 20837–20856, 1999.

Polvani, L. M. and Smith, K. L.: Can natural variability explain observed Antarctic sea ice trends? New modeling evidence from CMIP5, Geophys. Res. Lett., 40, 3195–3199, doi:10.1002/grl.50578, 2013.

Screen, J. A.: Sudden increase in Antarctic sea ice: Fact or artifact?, Geophys. Res. Lett., 38, L13 702, doi:10.1029/2011GL047553, 2011.

Sigmond, M. and Fyfe, J. C.: Has the ozone hole contributed to increased Antarctic sea ice extent?, Geophys. Res. Lett., 37, L18502, doi:10.1029/2010GL044301, 2010.

Thompson, D. W. J. and Solomon, S.: Interpretation of recent Southern Hemisphere climate change, Science, 296, 895–899, doi:10.1126/science.1069270, 2002.

Turner, J., Comiso, J. C., Marshall, G. J., Lachlan-Cope, T. A., Bracegirdle, T., Maksym, T., Meredith, M. P., Wang, Z. M., and Orr, A.: Non-annular atmospheric circulation change induced by stratospheric ozone depletion and its role in the recent increase of Antarctic sea ice extent, Geophys. Res. Lett., 36, L08502, doi:10.1029/2009GL037524, 2009.

Zhang, J. L.: Increasing Antarctic sea ice under warming atmospheric and oceanic conditions, J. Climate, 20, 2515–2529, doi:10.1175/JCLI4136.1, 2007.

Zunz, V., Goosse, H., and Massonnet, F.: How does internal variability influence the ability of CMIP5 models to reproduce the recent trend in Southern Ocean sea ice extent?, The Cryosphere, 7, 451–468, doi:10.5194/tc-7-451-2013, 2013.

Zwally, H. J., Comiso, J. C., Parkinson, C. L., Cavalieri, D. J., and Gloersen, P.: Variability of Antarctic sea ice 1979–1998, J. Geophys. Res., 107, 3041, doi:10.1029/2000JC000733, 2002.

Supplemental Discussion and Figures

S1 Detailed description of data and methods

Here we discuss the ice concentration fields analyzed in this study and the resulting time series of ice extent and ice area that we calculate.

S1.1 Ice concentration

The ice concentration data sets considered in this study are derived from passive microwave measurements from instruments flown on a series of satellites. The Scanning Multichannel Microwave Radiometer (SMMR) was flown on the NASA Nimbus 7 satellite and provided data between 26 October 1978 and 20 August 1987, with the Bootstrap sea ice concentration using the data between 1 November 1978 and 31 July 1987. SSMR measured radiances in 10 channels including 18.0H, 18.0V, 21.0V, 37.0H, and 37.0V; here the number refers to the frequency in GHz and the letter indicates vertical (V) or horizontal (H) polarization. Although the Nimbus 7 passed over both polar regions every day, the radiometer operated only on alternate days due to power limitations, leading to a temporal resolution of 2 days. SMMR was succeeded by the Special Sensor Microwave/Imager (SSM/I), which measured radiances every day in 7 channels including 19.3H, 19.3V, 22.2V, 37.0H, and 37.0V. SSM/I instruments were flown on a sequence of three Defense Meteorological Satellite Program (DMSP) satellites beginning in July 1987. For the Bootstrap sea ice concentration, data from the DMSP F8 satellite is used from 1 August 1987 until 2 December 1991, data from the DMSP F11 satellite is used from 3 December 1991 until 30 September 1995, and data from the DMSP F13 satellite is used from 1 October 1995 to 31 December 2007. The sensor transition that we focus on in this study is between the F8 and F11 platforms in December 1991. The Special Sensor Microwave Imager Sounder (SSMIS), which measures radiances in 24 different channels including 19.3H, 19.3V, 22.2V, 37.0H, and 37.0V, has been generating daily data from a Department of Defense satellite since 14 December 2006, with the Bootstrap sea ice concentration using data starting on 1 January 2008.

We consider both hemispheres in this Supplement. We focus on ice concentration data sets generated from the passive microwave radiance measurements using the Bootstrap algorithm, and in this Supplement we also consider data generated with the NASA Team algorithm. The Bootstrap algorithm uses data from the 19V, 37V, and 37H channels, and the NASA Team algorithm uses data from the 19H, 19V, and 37V channels. Both algorithms also draw on the 22V channel to filter out weather effects. The use of brightness temperature ratios in the NASA Team algorithm reduces errors due to surface temperature variations, but unlike the Bootstrap algorithm, the NASA Team algorithm is biased toward underestimating sea ice concentrations (Comiso et al., 1997). Both algorithms have empirically adjusted parameters that differ between the two hemispheres, and the parameters in the Bootstrap algorithm also vary on a daily basis.

Various steps go into processing the ice concentration data to intercalibrate across the transition from one sensor to another and to fill in missing or identifiably erroneous pixels. Although a number of brief data gaps exist, the instruments have provided data for at least 20 days of every month (10 days for SMMR) from November 1978 to present with the exception of December 1987 and January 1988, when the SSM/I instrument was turned off between 3 December 1987 and 13 January 1988 due to overheating issues.

The effective resolution (sensor footprint) of the microwave measurements vary as a function of frequency, with the resolution of the most coarse frequency used by the Bootstrap and NASA Team algorithms being approximately 40 km $\times$ 70 km. However, all concentrations are derived from daily passive microwave brightness temperatures mapped onto a polar stereographic grid with a nominal resolution of 25 $\times$ 25 km.

A region around each pole is not imaged due to the inclination angle of the satellite orbit. This hole is located poleward of 84.5°N for SMMR and 87.2°N for SSM/I. SSMIS has a slightly smaller hole than SSM/I, but the SSM/I hole is used for SSMIS to simplify processing.

The Bootstrap data is processed at NASA Goddard Space Flight Center and distributed by the National Snow and Ice Data Center (NSIDC) (Comiso, 2000), and we acquired from NSIDC the daily Bootstrap ice concentration data sets from before (Version 1) and after (Version 2) the entire data set was reprocessed in September 2007 using an updated Bootstrap algorithm (see Sect S1.3).

S1.2 Ice extent and ice area

We calculate the daily ice area in a given hemisphere from the gridded ice concentration field in both Bootstrap versions by summing the surface area of all grid cells weighted by the ice concentration. Following a standard convention (e.g., Cavalieri et al., 1999), we exclude grid cells with ice concentration less than 15% due to wind roughening and other weather filtering issues near the ice edge.

A more common measure of the hemispheric sea ice cover is the ice extent, which is defined as the sum of the surface area of all pixels with ice concentration above a specified threshold, normally taken to be 15% since this has been found to correspond with the ice edge estimated using aircraft measurements (Cavalieri et al., 1991). In other words, the ice extent includes the area of leads within grid cells that have ice concentration above 15%, whereas the ice area does not. We calculate the daily ice extent for both Bootstrap versions following this convention, and ice extent is used exclusively in the main paper. An advantage of using ice extent rather than ice area is that ice extent is less sensitive to errors in the ice concentration field, such as those associated with the misidentification of surface melt ponds during the summer as open ocean. Two disadvantages of using ice extent rather than ice area are that ice extent is less physically relevant, since it includes the area of patches of open water within the ice pack, and that ice extent depends more on pixel resolution.

In the Arctic, we mask lakes from the ice concentration field and assume the hole around the pole has 100% ice concentration; note that this causes a small erroneous decrease in Arctic sea ice area in 1987 associated with the decrease in the radius of the hole between SMMR and SSM/I.

We compute daily ice extent and then take monthly averages, rather than computing the ice extent from monthly averaged ice concentration fields, which avoids biases associated with the merging of temporal and spatial averages. We average the ice extent and ice area over all days in each month with data, with the exception of December 1987 and January 1988, when there is limited data as described above. These two months are filled using linear interpolation between the same month in the previous year and the following year. The result is a monthly time series of ice extent and ice area for each Bootstrap version in each hemisphere.

We also include analysis of an approximation to Version 1 ice extent and ice area in the Antarctic only, which we call "Version 1B". The Version 1B ice extent time series is identical to Version 2 except that $0.16 \times 10^6\,\mathrm{km}^2$ is removed from all months after December 1991. The Version 1B ice area time series is generated similarly, except that a somewhat somewhat smaller value of $0.12 \times 10^6\,\mathrm{km}^2$ is removed from all months after December 1991. In both cases, the size of the step function was chosen to match the Version 1 trend for the range of endpoints plotted in Fig. 1b (see Fig. S5c,g).

For the NASA Team algorithm, we use a time series of monthly-mean ice extent and ice area downloaded from the NSIDC "Sea Ice Index" archive (Fetterer et al., 2002). We interpolate over the months 12/1987 and 1/1988, as described above for the Bootstrap algorithm, and we add the area of the hole around the pole to the Arctic sea ice area.

The four time series of monthly-mean ice extent and ice area in each hemisphere all begin in November 1978, but they end at different times. The Bootstrap Version 1 data set ends in December 2004, the Bootstrap Version 1B and Version 2 data sets ends in December 2012, and the NASA Team data set ends in August 2013 (including near-real-time data during the months of 2013 because final NASA Team data was not yet available at the time of analysis).

S1.3 Documentation of update from Bootstrap Version 1 to Version 2

A separate satellite passive microwave data set is available from the Advanced Microwave Scanning Radiometer for the Earth Observing System (AMSR-E), which is flown on the NASA Aqua satellite. AMSR-E provided data from 19 June 2002 until 4 October 2011, when an antenna problem caused the sensor to stop operating. Compared to SSM/I, AMSR-E has finer spatial resolution and provides data over a wider range of microwave frequencies.

The Bootstrap algorithm was revised and a new version of the NASA Team algorithm (NASA Team 2) was created for use with the AMSR-E data (Comiso et al., 2003). Considering four years of overlap between AMSR-E and SSM/I (2002-2006), ice covers estimated with the Bootstrap algorithm from both satellites, as well as NASA Team SSM/I results, were all found to be in fairly good agreement overall for both hemispheres (Comiso and Parkinson, 2008; Parkinson and Comiso, 2008).

Nonetheless, Comiso and Nishio (2008) introduced an adjustment to the Bootstrap data set for consistency between the two instruments, after which Comiso and Nishio (2008) found that the 1978–2006 record that had AMSR-E data during 2002–2006 had a trend of $10.8 \times 10^3\,\mathrm{km}^2\,\mathrm{yr}^{-1}$, nearly identical to the 1978–2006 trend in the original SMMR and SSM/I Bootstrap data set which they found to be $10.9 \times 10^3\,\mathrm{km}^2\,\mathrm{yr}^{-1}$.

Other adjustments to the Bootstrap algorithm were also documented around this time. The Bootstrap algorithm formerly used only the 19V and 37V channels in the Antarctic, whereas it uses the 19V, 37V, and 37H channels in the Arctic where the fraction of first-year ice is smaller. The algorithm was updated to use the 19V, 37V, and 37H channels in the Antarctic, as in the Arctic, in order to remove a small negative bias identified in the ice concentration (Comiso, 2007).

After these changes were made to the Bootstrap algorithm, the entire data set was reprocessed and updated from Version 1 to Version 2 on the NSIDC website (Comiso, 2000).

We note that there appears to be some ambiguity in the Bootstrap data set version control. For example, the "Version History" in the NSIDC online documentation (Comiso, 2000) mentions the adjustment in Version 2 for consistency with AMSR-E but does not mention the change in input channels. However, the more extensive documentation linked from the website (Comiso, 2007), which does not explicitly mention version numbers, refers to the change in input parameters as "the biggest change in the revised version of the Bootstrap data set".

S2 Structure of trends in both hemispheres

Here we examine further details of the sea ice trends that are not included in the main paper. We examine ice extent as well as ice area. For comparison with the two Bootstrap versions, we consider ice cover estimated using the NASA Team algorithm. We also consider the ice extent and ice area from the same three data sets in the Arctic.

S2.1 Monthly ice extent and ice area

We focus on anomalies from the mean seasonal cycle in each record (Fig. S1). The difference between the two Bootstrap versions and the NASA Team ice extent is plotted in Fig. S2b,c in order to see whether it allows us to discern which of the two Bootstrap versions had a spurious jump in December 1991. These differences are too large and noisy to isolate any readily discernible change around December 1991. In Fig. S2c, however, there appears to be a rather subtle tendency for low values before December 1991 and high values afterwards, similar to Fig. S2a. This would imply an error in Version 2, but further statistical analyses would be required to determine whether this difference, which is largely masked by month-to-month variability, is statistically meaningful.

It should be noted that Figs. S2b,c display an apparent jump from high values before the 1987 sensor transition to low values afterwards, implying a possible difference between NASA Team and the two Bootstrap versions in the intercalibration across the transition from SMMR to SSM/I.

Similar to ice extent, the difference in ice area between Bootstrap Version 2 and Version 1 shows a clear transition in December 1991 (Fig. S2d). But for ice area, as for ice extent, the difference between each Bootstrap version and the NASA Team data is too large and variable to readily discern which Bootstrap data set experienced the spurious jump (Fig. S2e,f): there is no readily discernible step in December 1991 that stands out above the month-to-month variability. However, there appears to be a rather subtle transition from low to high values at the 1991 sensor transition in Fig. S2f, although more work would be needed to determine whether it is statistically meaningful.

Because similar algorithms are used in both hemispheres, we also consider ice extent and ice area anomalies in the Arctic (Fig. S3). A notable feature of the ice extent and ice area anomalies in all three data sets is the onset of large-amplitude low-frequency variability beginning in 2007 (Fig. S3b,d). This may be attributable to issues of coastline geometry causing the ice extent seasonal cycle amplitude to increase (Eisenman, 2010).

A number of changes in the Arctic sea ice extent data sets approximately coincide with sensor changes. A bias in the difference between the Bootstrap data sets appears to be introduced at the 1987 sensor change and then approximately compensated for at the 1992 sensor change (Fig. S4a). Similarly, a persistent offset between the NASA Team record and the two Bootstrap records appears to be introduced at the sensor change in 1987 (Figs. S4b,c). Furthermore, the NASA Team ice extent briefly drops considerably below both Bootstrap versions around the 1987 sensor change and briefly rises considerably above them around the 1995 sensor change, causing noticeable spikes in the comparison between NASA Team and either Bootstrap version that approximately coincide with the times of the sensor changes (Figs. S4b,c).

The Arctic sea ice area also shows a spike that approximately coincides with the 1987 sensor change (Figs. S4e,f). There appears to also be a rather subtle tendency for Bootstrap Version 2 to be higher than Version 1 after the 1992 sensor change (Fig. S4d).

Overall, we do not see a compelling indication in the Arctic ice extent or ice area data whether Bootstrap Version 1 or Version 2 is more likely to contain errors in both hemispheres.

S2.2 Ice extent and ice area trends

We examine the trend in the Bootstrap Version 1 and Version 2 data, as well as the NASA Team data, in both hemispheres. It is instructive to compare the differences between the data sets with the reported error bar on the trend, which provides an indication of the significance of the difference in trend between Version 1 and Version 2. Ice extent trends are often reported with error bars based on the 68% linear regression confidence interval using monthly data (e.g., Comiso and Steffen, 2001; Comiso, 2003; Comiso and Nishio, 2008; Comiso, 2010), which is an estimate of the error associated with natural variability about the trend. The IPCC AR4 and IPCC AR5 instead use a 90% linear regression confidence interval, with the IPCC AR4 using annual data and the IPCC AR5 using monthly data (see Appendix A1 of main text). Hence we plot both the 68% and 90% confidence intervals, as well as the 99% confidence interval, for monthly and annual data (Figs. S5-S8). We also compare trends in both Bootstrap data sets with the values reported in the two IPCC reports in Table S1.

In the Antarctic, the Bootstrap Version 2 ice extent trend is well outside the 90% confidence interval of the Bootstrap Version 1 trend and near the edge of the 99% confidence interval for all plotted record endpoints (Fig. S5b). Similar features apply to the trend in ice area: Bootstrap Version 2 is near the edge of the 99% confidence interval of Bootstrap Version 1 (Fig. S5f).

The trend in the Bootstrap Version 2 ice extent (Fig. S5a) agrees fairly closely with the NASA Team data (Fig. S5d), whereas Bootstrap Version 1 does not (Fig. S5b), implying that an error in the Bootstrap data set may have been corrected between Version 1 and Version 2. In contrast, however, the trend in NASA Team ice area (Fig. S5h) agrees closely with Bootstrap Version 1 (Fig. S5f) but not with Bootstrap Version 2 (Fig. S5e), implying instead that Version 2 introduced an error into the Bootstrap data set that did not exist in Version 1. This could be related to the previously discussed low bias in NASA Team ice concentration (e.g., Comiso et al., 1997), which could plausibly affect the ice area trend.

However, the comparison is reversed in the Arctic. The trend in Arctic sea ice area agrees closely between both Bootstrap versions and NASA Team, whereas the trend in Arctic sea ice extent differs substantially between each of the three records (Fig. S7). Interestingly, the trend in Bootstrap

Version 2 Arctic sea ice extent falls near the edge of the 99% regression confidence interval of the NASA Team trend (Fig. S7c): If both current data sets are seen as reliable estimates of the sea ice cover, then this indicates that the regression confidence interval substantially underestimates the uncertainty in the Arctic sea ice trend by failing to account for errors associated with the satellite retrieval algorithm.

In the Arctic, the trend in sea ice extent differs between Version 1 and Version 2 (Fig. S7), as in the Antarctic. However, in contrast to the Antarctic, this change is relatively small compared with the changes in the linear trend during the past decade associated with the actual acceleration of the ice retreat.

It is interesting in Fig. S7 that for ice extent and ice area in all the data sets, the trend appears to remain relatively constant before ∼2005, then to drop rapidly, and then to drop more slowly after ∼2007, although the extent to which these features are statistically meaningful is not investigated here.

The trends in both hemispheres using annual data (Figs. S6,S8) resemble the trends from monthly data (Figs. S5,S7), except that the error bars are typically approximately twice as large.

S2.3 Seasonal structure of trends

There is not a strong seasonal structure to the trend in the Antarctic sea ice cover in any of the data sets considered here (Fig. S9). Although the trend is larger in March/June than in September/December for many record endpoints in all three ice extent data sets, both Bootstrap Version 2 and NASA Team produce ice extent and ice area trends that are smallest in March for the most recent record endpoints. Other studies that have reported the trend to be largest in Austral summer have measured the trend in percent per decade, dividing the trend by the mean value for each month and thereby introducing a strong seasonality associated with the denominator (e.g., Turner and Overland, 2009).

The seasonal uniformity in the Antarctic is in contrast with the Arctic (Fig. S10), where the retreat is fastest in boreal late summer, a feature that has been attributed to the configuration of continents in the Arctic (Eisenman, 2010).

S2.4 Spatial structure of trends

The spatial structure of the trends in both Bootstrap versions is compared in Fig. S11. We consider the change between the late 1980s and the late 1990s in order to focus on the shift that occurred in December 1991 (Fig. 2). Both versions have nearly identical spatial patterns of the change for all seasons during this time period, and the first row of Fig. S11 is nearly indistinguishable from the second row. However, it is the relatively small difference between large regional expansions and contractions that give rise to the trend in total ice extent or ice area. Considering the difference between the two versions (lowest row of Fig. S11), Version 2 changes in a more positive way than Version 1 during this period in most locations and seasons. This difference is relatively uniform spatially and among seasons, in contrast with the strongly spatially-varied trend in each data set individually and consistent with a sensor intercalibration issue explaining the difference between the versions.

References

Cavalieri, D. J., Crawford, J. P., Drinkwater, M. R., Eppler, D. T., Farmer, L. D., Jentz, R. R., and Wackerman, C. C.: Aircraft active and passive microwave validation of sea ice concentration from the defense meteorological satellite program special sensor microwave imager, J. Geophys. Res., 96, 21 989–22 008, doi:10.1029/91JC02335, 1991.

Cavalieri, D. J., Parkinson, C. L., Gloersen, P., Comiso, J. C., and Zwally, H. J.: Deriving long-term time series of sea ice cover from satellite passive-microwave multisensor data sets, J. Geophys. Res., 104, 15 803–15 814, doi:10.1029/1999JC900081, 1999.

Comiso, J. C.: Bootstrap Sea Ice Concentrations from Nimbus-7 SMMR and DMSP SSM/I-SSMIS. Version 2, Updated 2012, National Snow and Ice Data Center, Boulder, CO, USA, available at: http://nsidc.org/data/nsidc-0079.html (last access: 30 September 2013), 2000.

Comiso, J. C.: Large scale characteristics and variability of the global sea ice cover, in: Sea Ice – An Introduction to its Physics, Biology, Chemistry and Geology, Blackwell Scientific Ltd., Oxford, UK, 112–142, 2003.

Comiso, J. C.: Enhanced Sea Ice Concentrations from Passive Microwave Data. National Snow and Ice Data Center, Boulder, CO, USA, available at: http://nsidc.org/data/docs/daac/nsidc0079_bootstrap_seaice/docs/Bootstrap_Algorithm_Revised07.pdf (last access: 30 September 2013), 2007.

Comiso, J. C.: Variability and trends of the global sea ice cover, in: Sea Ice, 2nd edn., Wiley-Blackwell, Oxford, UK, 205–246, 2010.

Comiso, J. C. and Nishio, F.: Trends in the sea ice cover using enhanced and compatible AMSR-E, SSM/I, and SMMR data, J. Geophys. Res., 113, C02S07, doi:10.1029/2007JC004257, 2008.

Comiso, J. C. and Parkinson, C. L.: Arctic sea ice parameters from AMSR-E data using two techniques and comparisons with sea ice from SSM/I, J. Geophys. Res., 113, C02S05, doi:10.1029/2007JC004255, 2008.

Comiso, J. C. and Steffen, K.: Studies of Antarctic sea ice concentrations from satellite data and their applications, J. Geophys. Res., 106, 31361–31385, doi:10.1029/2001JC000823, 2001.

Comiso, J. C., Cavalieri, D. J., Parkinson, C. L., and Gloersen, P.: Passive microwave algorithms for sea ice concentration: A comparison of two techniques, Remote Sens. Environ., 60, 357–384, 1997.

Comiso, J. C., Cavalieri, D. J., and Markus, T.: Sea ice concentration, ice temperature, and snow depth using AMSR-E data, IEEE Transactions On Geoscience Remote Sensing, 41, 243–252, doi:10.1109/TGRS.2002.808317, 2003.

Eisenman, I.: Geographic muting of changes in the Arctic sea ice cover, Geophys. Res. Lett., 37, L16 501, doi:10.1029/2010GL043741, 2010.

Fetterer, F., Knowles, K., Meier, W., and Savoie, M.: Sea ice index, Updated 2012, National Snow and Ice Data Center, Boulder, CO, USA, available at: http://nsidc.org/data/g02135.html (last access: 1 July 2013), 2002.

IPCC: Climate Change 2007: The Physical Science Basis. Contribution of Working Group I to the Fourth Assessment Report of the Intergovernmental Panel on Climate Change, edited by: Solomon, S., Qin, D., Manning, M., Chen, Z., Marquis, M., Averyt, K. B., Tignor, M., and Miller, H. L., Cambridge University Press, Cambridge, United Kingdom and New York, NY, USA, 2007.

Parkinson, C. L. and Comiso, J. C.: Antarctic sea ice parameters from AMSR-E data using two techniques and comparisons with sea ice from SSM/I, J. Geophys. Res., 113, C02S06, doi:10.1029/2007JC004253, 2008.

Screen, J. A.: Sudden increase in Antarctic sea ice: Fact or artifact?, Geophys. Res. Lett., 38, L13 702, doi:10.1029/2011GL047553, 2011.

Turner, J. and Overland, J.: Contrasting climate change in the two polar regions, Polar Res., 28, 146–164, doi:10.1111/j.1751-8369.2009.00128.x, 2009.

Table S1. Trends for different time periods and data sets, including 90% regression confidence interval error bars, in units of $10^3\,\mathrm{km}^2\,\mathrm{yr}^{-1}$. Annual trends are calculated using January–December averages for each year. The slight differences between trends reported in the IPCC reports and those computed here with the matching Bootstrap version are expected to arise due to issues including rounding errors and slight differences in the data sets and methodology such as how missing data is treated and how ice extent is calculated from the gridded ice concentration fields.

	11/1978–12/2005 monthly	1979–2005 annual	11/1978–12/2012 monthly	1979–2012 annual
IPCC AR4		5.6 ± 9.2		
Bootstrap v1B	4.9 ± 4.5	5.2 ± 8.0	10.3 ± 3.5	10.5 ± 6.7
IPCC AR5			16.5 ± 3.5	
Bootstrap v2	13.7 ± 4.5	14.1 ± 8.2	16.9 ± 3.5	17.2 ± 6.6

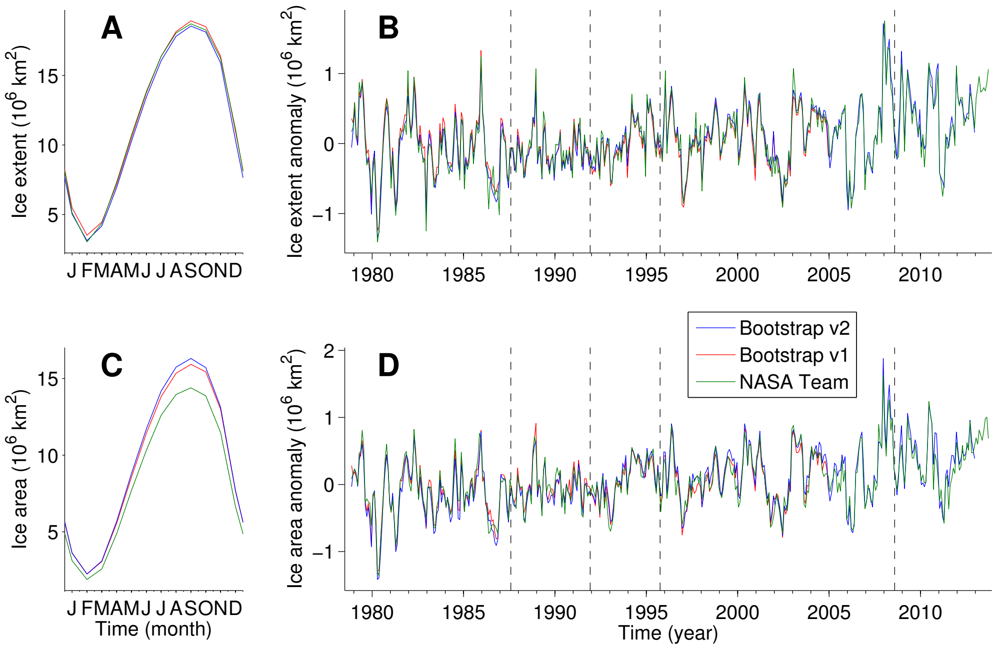

Fig. S1. (A) Mean seasonal cycle of Antarctic sea ice extent during 1979–2004 and (B) time series of monthly-mean anomalies from the mean seasonal cycle for both versions of the Bootstrap data as well as the NASA Team data. (C)-(D) Same, but for ice area rather than ice extent. Transitions between sensors are indicated by vertical dashed lines (see Sect. S1.1).

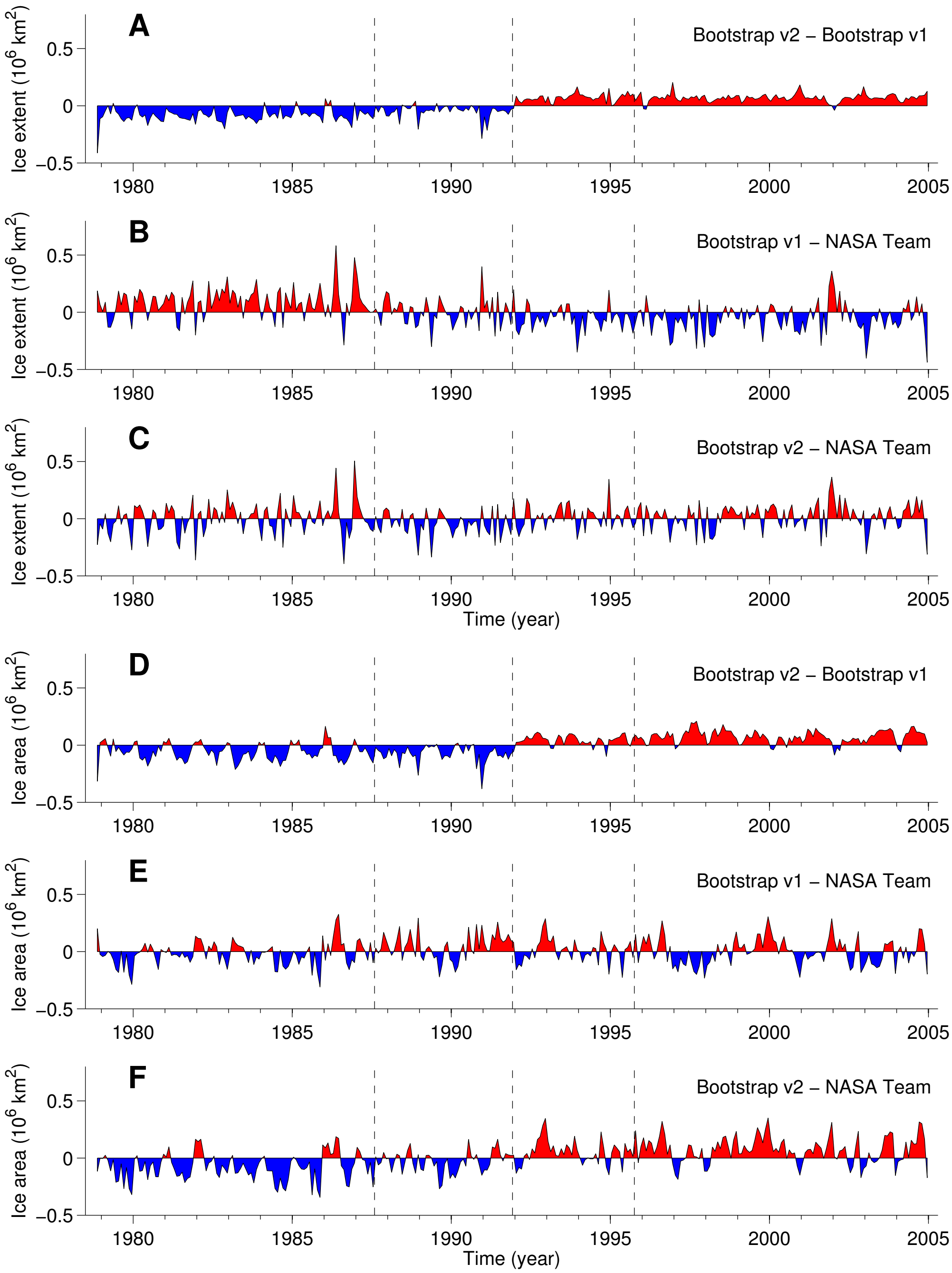

Fig. S2. Antarctic sea ice anomalies from the 1979–2004 mean seasonal cycle. (A-C) Difference between monthly-mean Antarctic sea ice extents computed using Bootstrap Version 1, Bootstrap Version 2, and NASA Team data sets. Data sets are indicated in the top right corner of each panel. Panel A is equivalent to Fig. 2. (D-F) Same, but for ice area rather than ice extent. Transitions between sensors are indicated by vertical dashed lines (see Sect. S1.1). The plotted time interval is the period during which Bootstrap Version 1 data is available.

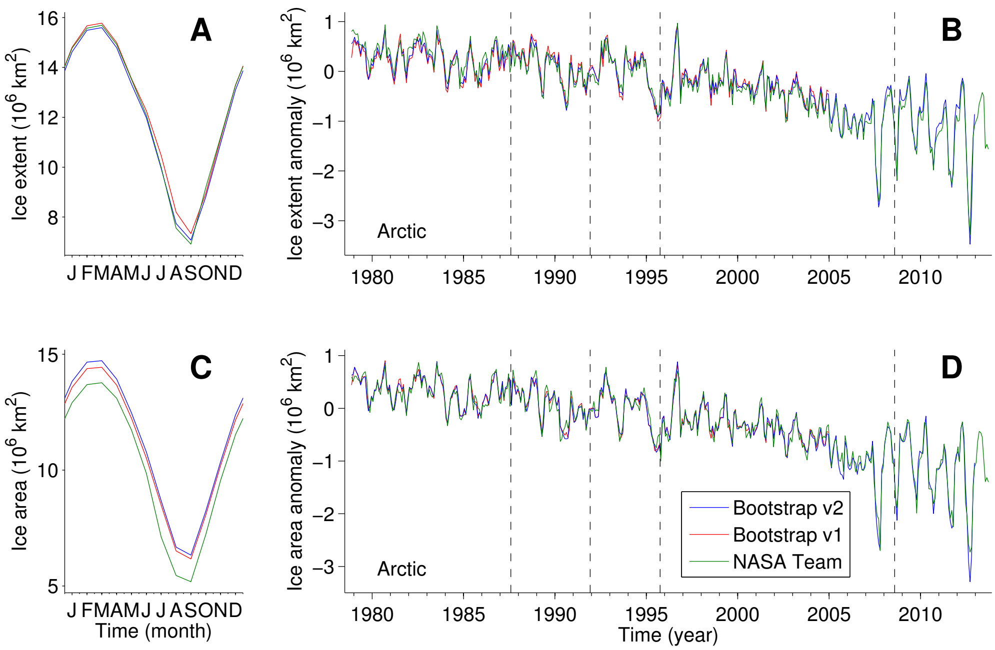

Fig. S3. As in Fig. S1, but for the Arctic.

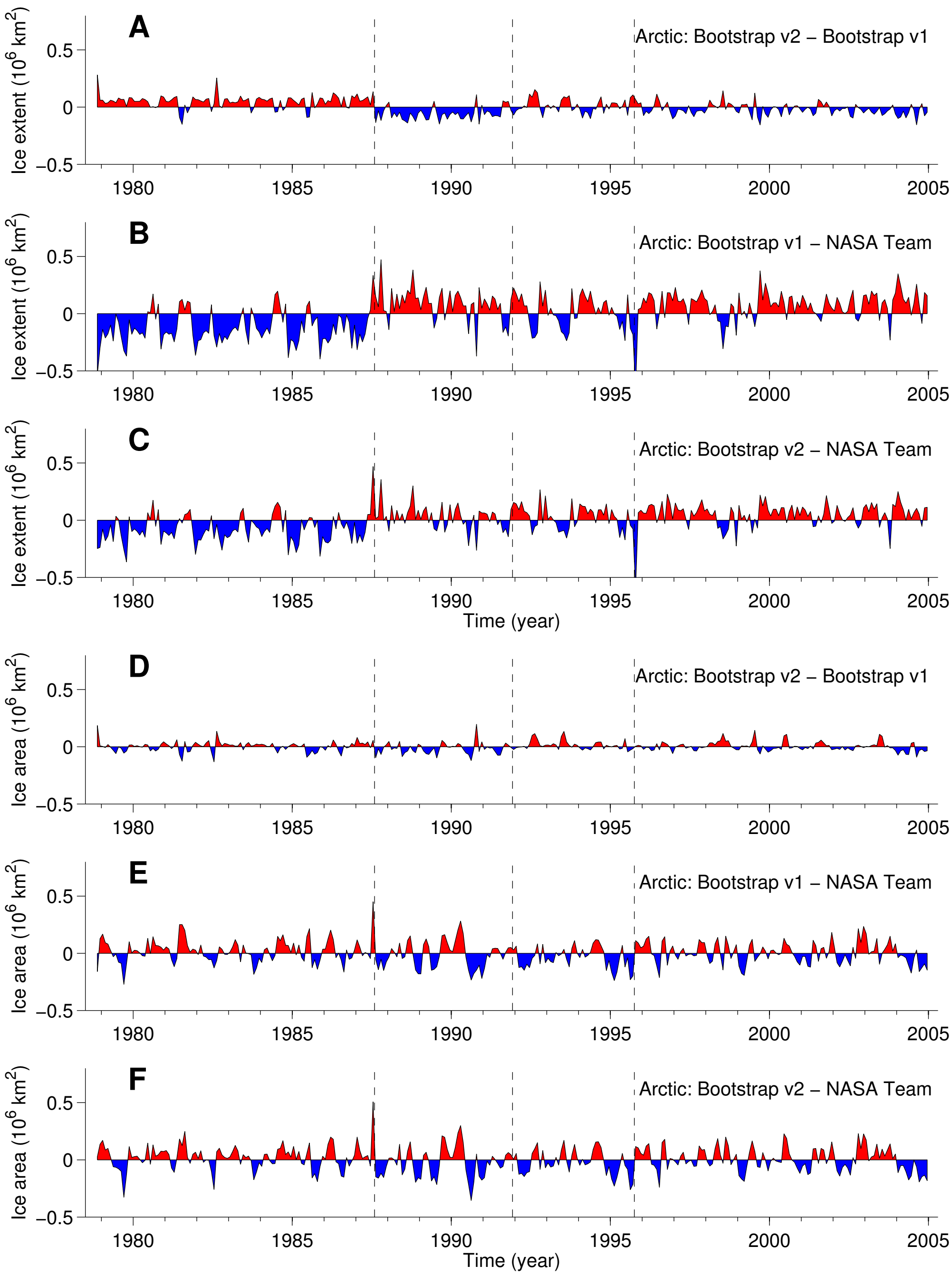

Fig. S4. As in Fig. S2, but for the Arctic.

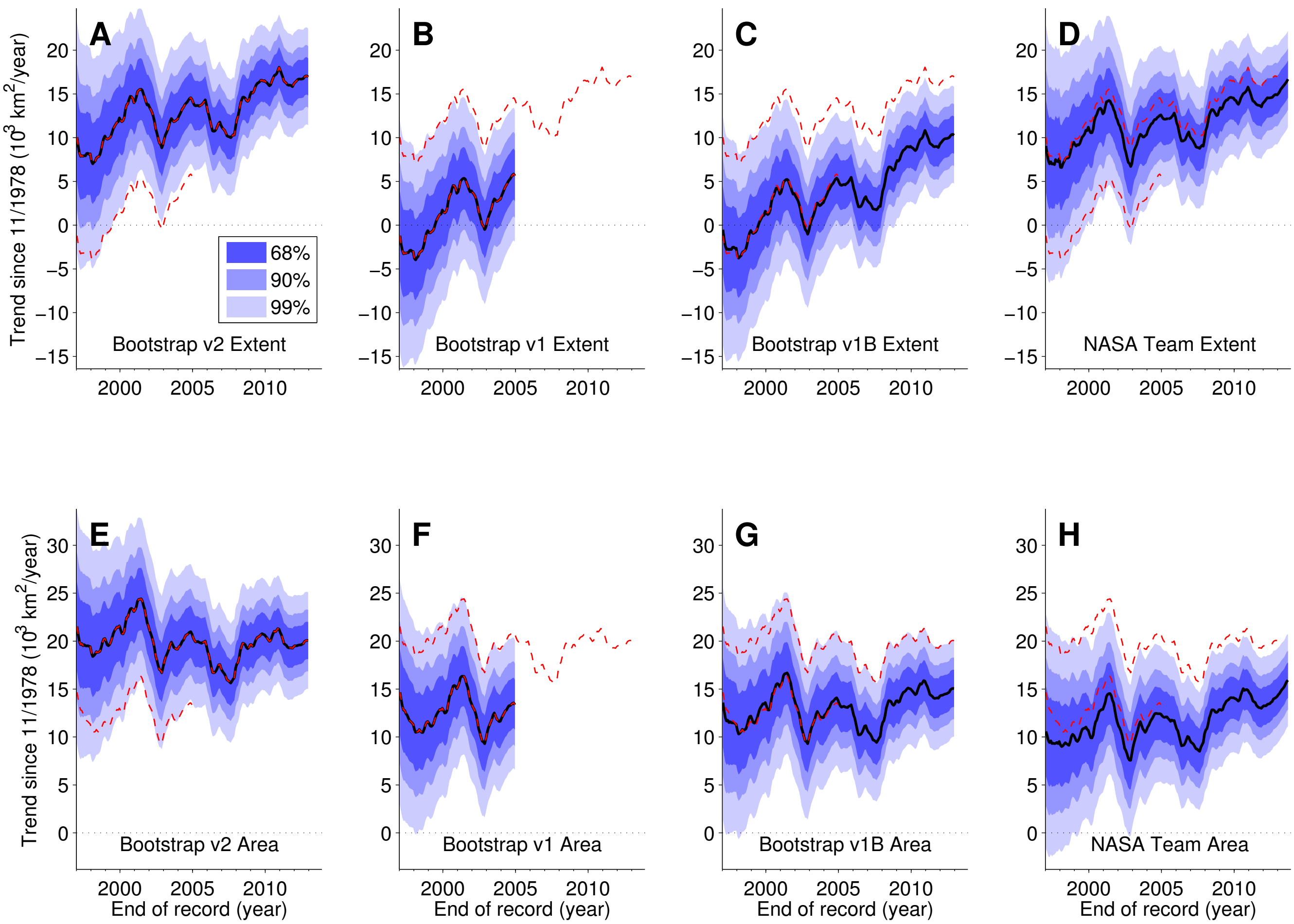

Fig. S5. Trends in Antarctic sea ice extent (top) and area (bottom) using Version 1, Version 1B, and Version 2 of the Bootstrap data set, as well as the NASA Team data set, for a range of record endpoints. Shades of blue indicate the 68% regression confidence interval (which is often used to represent the trend error bar in published studies), the 90% confidence interval (which is used to represent the error bar in the IPCC reports), and the 99% confidence interval. The trends computed using Version 1 and Version 2 of the Bootstrap data set (red dashed lines) are repeated across each row for comparison.

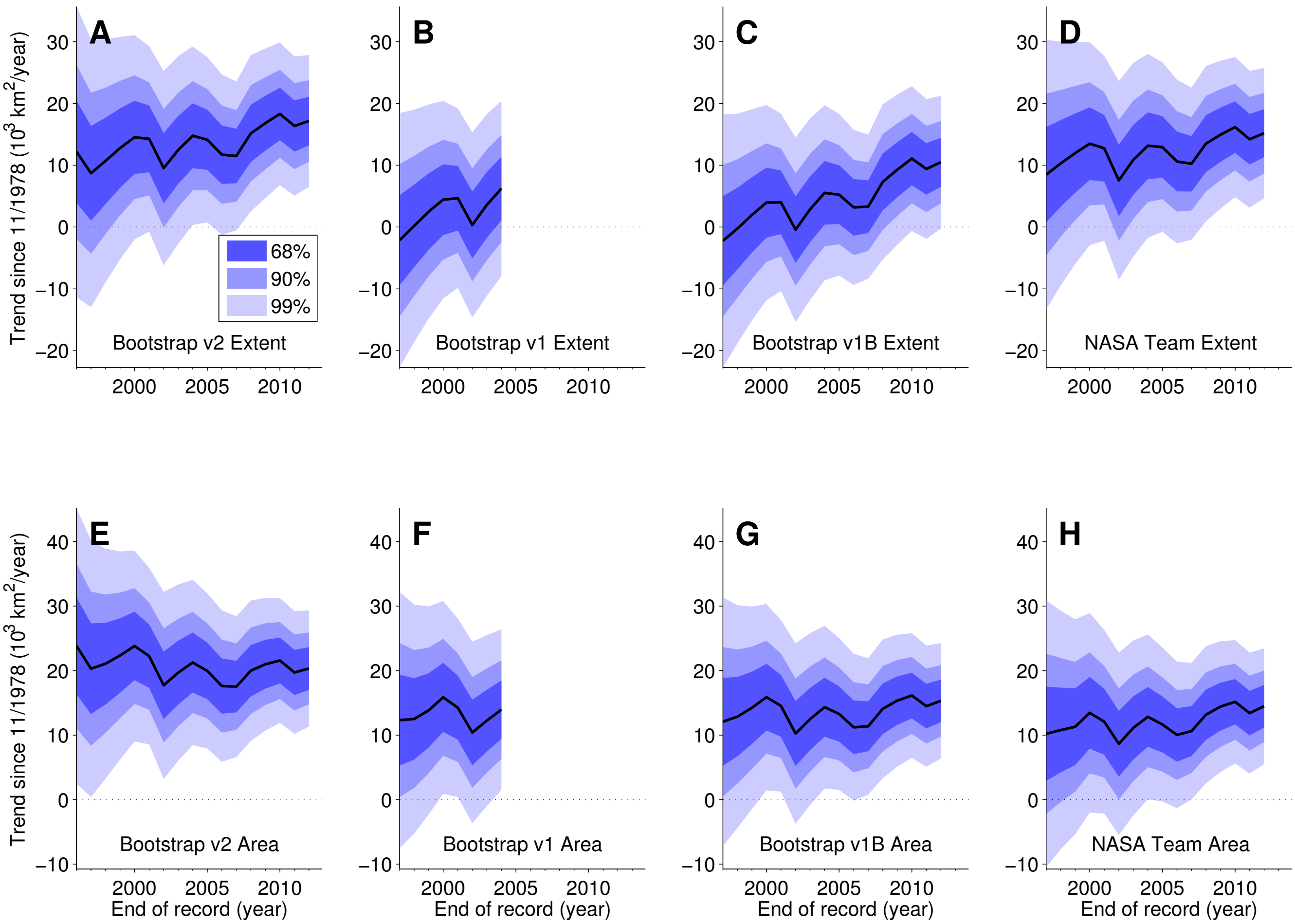

Fig. S6. As in Fig. S5, but using annual data. Note that the horizontal axis range is shifted compared with Fig. S4. This is because, for example, the trend in the data set that goes to the end of 2005 is plotted above the 2005 tick in this figure but above December 2005 (near the 2006 tick) in Fig. S4.

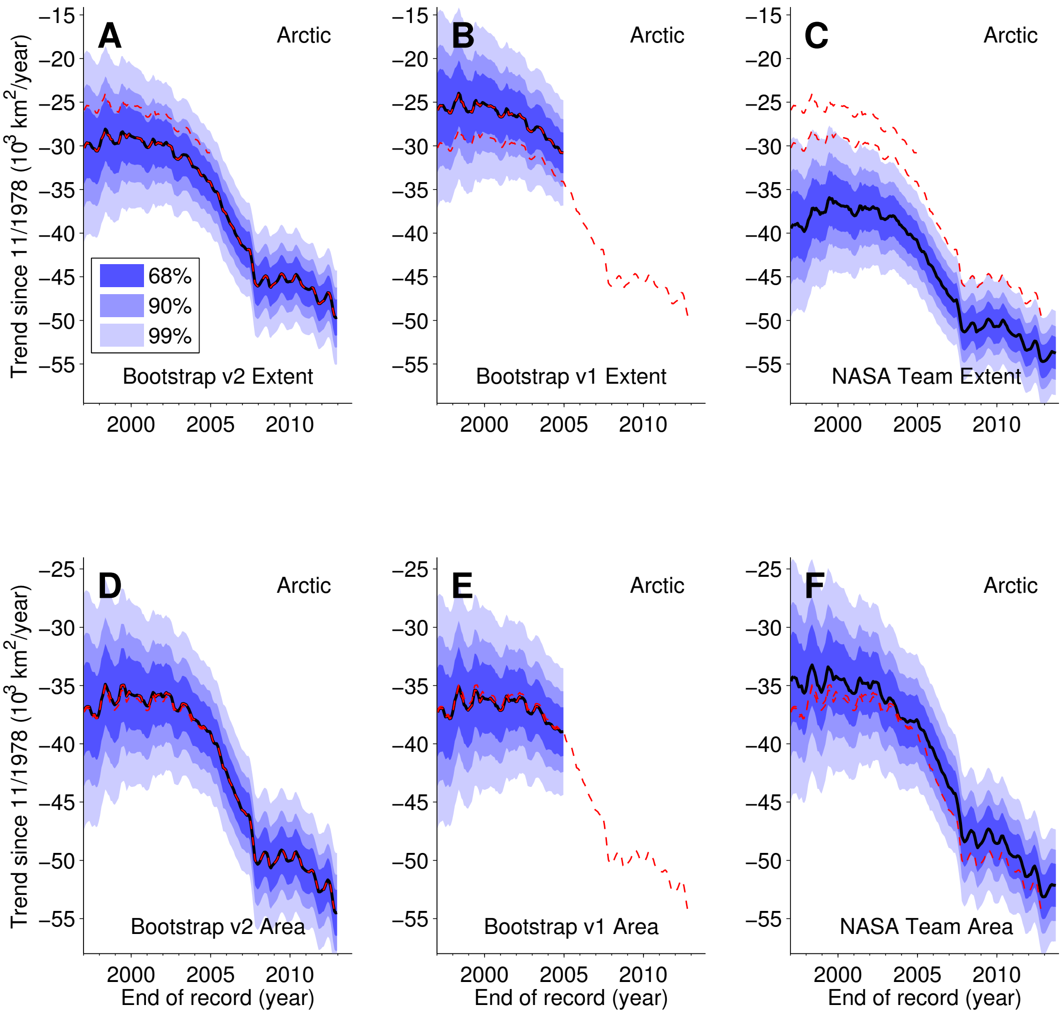

Fig. S7. As in Fig. S5, but for the Arctic.

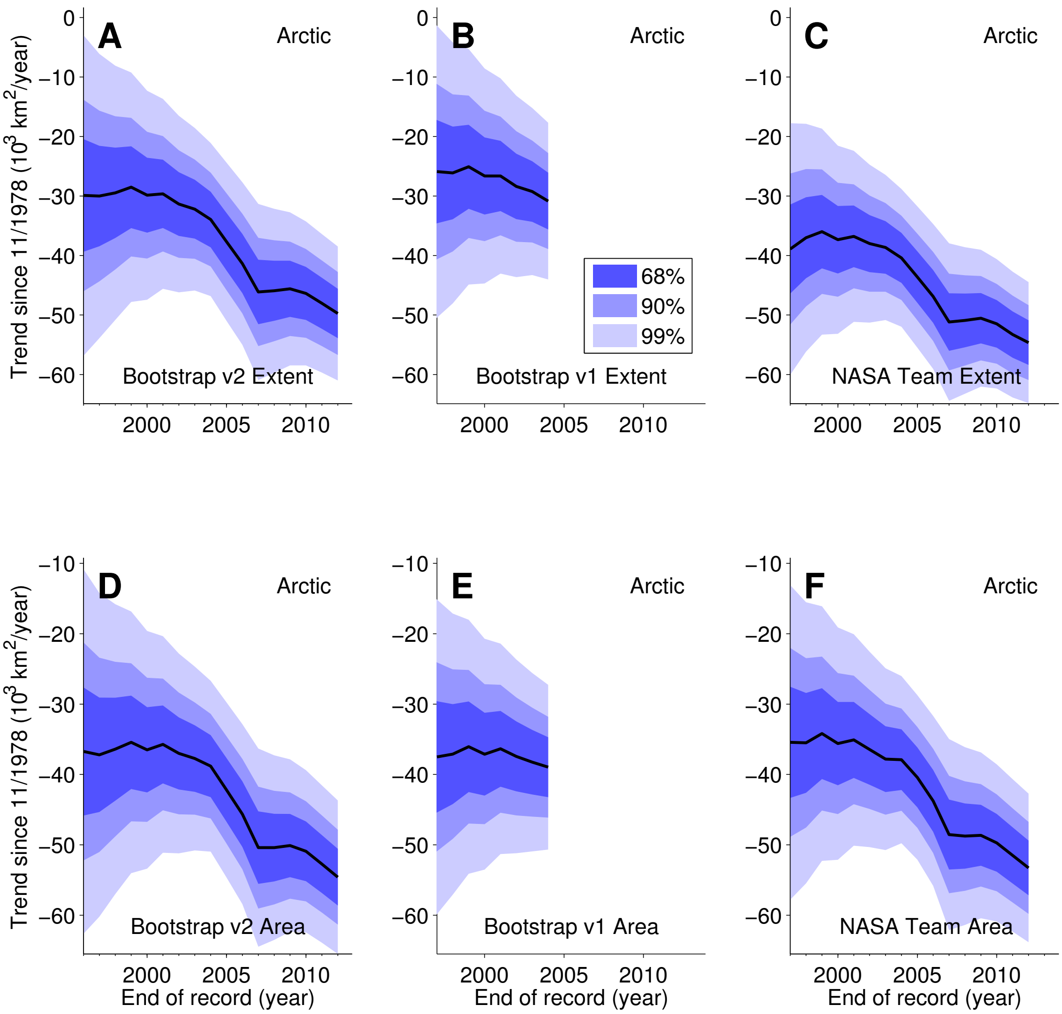

Fig. S8. As in Fig. S6, but for the Arctic.

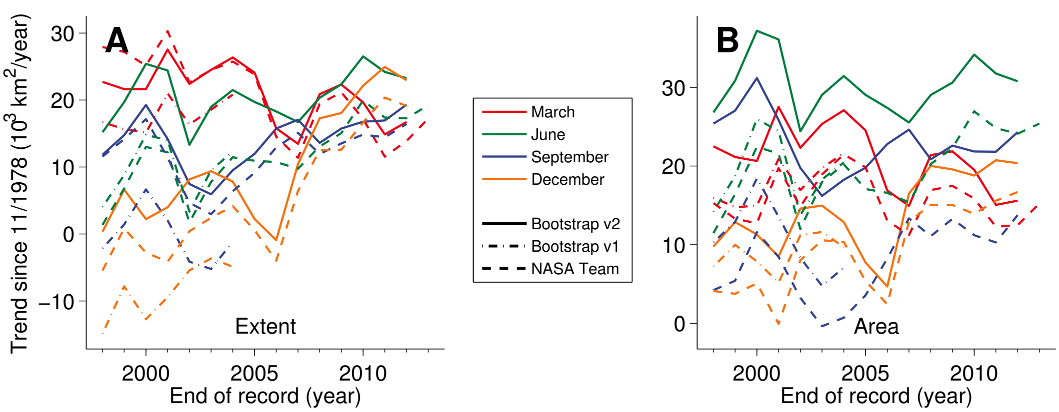

Fig. S9. Seasonal structure of trends in Antarctic (A) ice extent and (B) ice area. Here the trends are computed using only every March (red), June (green), September (blue), or December (orange) for a range of record endpoints. Results are plotted for Version 2 of the Bootstrap data set (solid), Version 1 of the Bootstrap data set (dot-dash), and the NASA Team data set (dash).

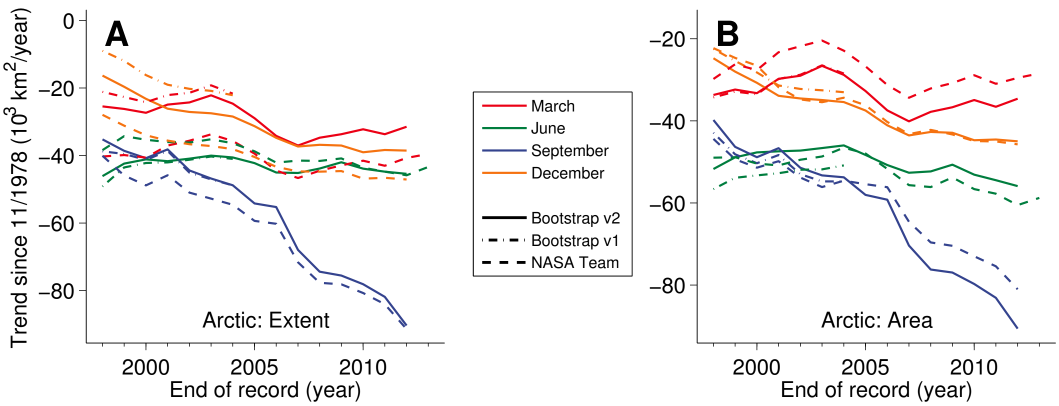

Fig. S10. As in Fig. S9, but for the Arctic.

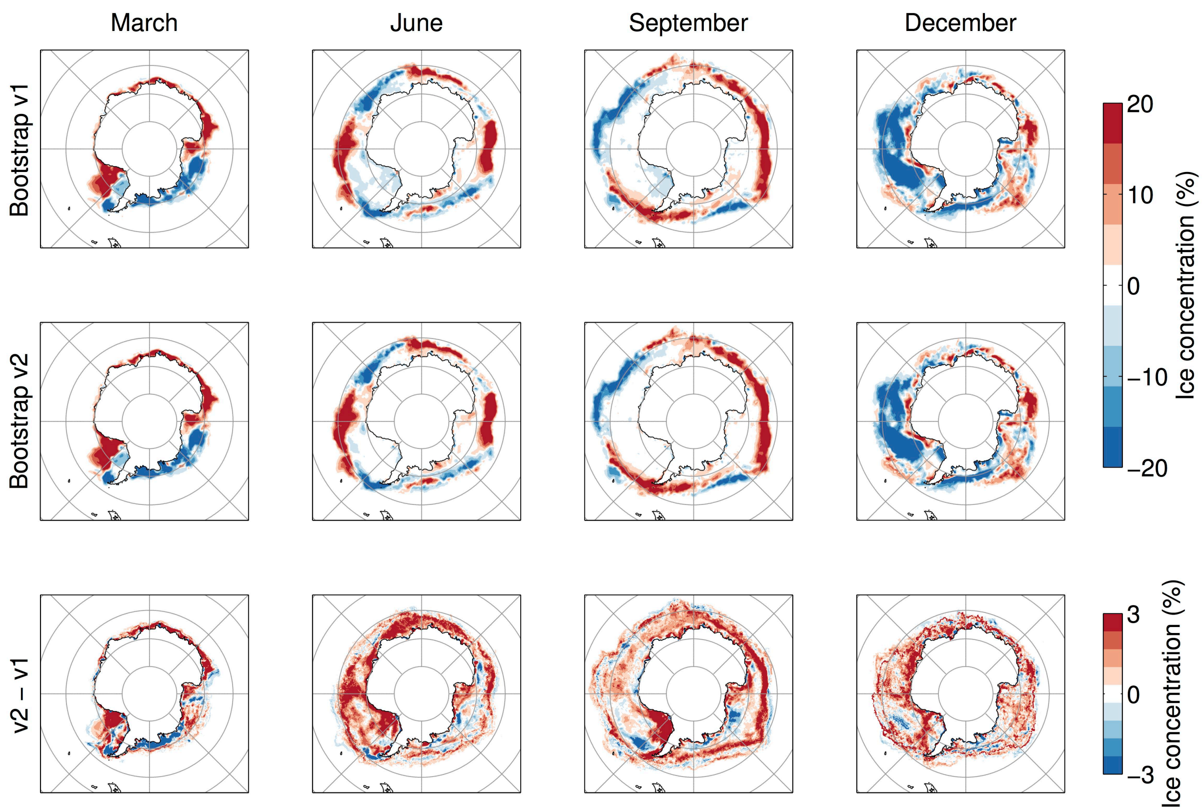

Fig. S11. Spatial structure of changes in Antarctic sea ice cover. (Top row) Change between late 1980s and late 1990s, calculated as the mean during 1985–1989 subtracted from the mean during 1995–1999, in the Bootstrap Version 1 data set. (Middle row) Same, but for the Bootstrap Version 2 data set. (Bottom row) Difference between Bootstrap versions, calculated as Version 2 minus Version 1. Each column represents a different month.